Internal Solitary Waves of Depression in Rapidly Varying Topography

Hooi Mun Hoe[1], Wei King Tiong[1,*], Kim Gaik Tay[2], San Nah Sze[1], Kang Leng Chiew[1]

[1] Faculty of Computer Science and Information Technology, Universiti Malaysia Sarawak, 94300 Kota Samarahan, Sarawak, Malaysia
[2] Department of Communication Engineering, Faculty of Electric and Electronic, Universiti Tun Hussein Onn Malaysia, 86400 Parit Raja, Johor, Malaysia

ARTICLE INFO	ABSTRACT
	Internal solitary waves have been observed in oceans all over the world. This paper looks at the effect of rapidly varying topography on the propagation of internal solitary waves in the framework of the variable-coefficient extended Korteweg-de Vries equation. We consider internal solitary wave is propagating in a two-layer fluid system. Here we let the depth of the upper layer to be smaller than the depth of lower layer such that initially an internal solitary wave of negative polarity is generated. The governing equation is solved numerically using the method of lines. Numerical results show that under the influence of variable topography, internal solitary waves would fission into few smaller solitary waves, an undular bore is generated for some time before transforms into a radiation wave or the internal solitary wave loses its amplitude when propagates over a sharply varying slope.

1. Introduction

Internal solitary waves are nonlinear waves usually formed from tide-topography interaction [1], density-stratified fluid [2] and wind force [3, 4]. They often propagate horizontally at the interface of two different density layers, where each layer has different constant buoyancy density existing in the oceanic pycnocline (see Figure 1).

Internal waves can be found mostly in fjords [5], straits [6], continental shelves [7- 9] and coastal areas e.g. in the Andaman Sea [10], Sulu Sea [11, 12] and South China Sea region [13-16]. A recent study in the area of northern South China Sea recorded that the amplitude of an extreme internal solitary wave could reach up to 240 meters with a peak velocity of 2.55 ms^{-1} while propagating at the bottom depth of 3847 meters [17]. With these characteristics of internal solitary waves, they can transport large tidal energy over a long distance such that they could bring substantial shocks to

---

* Corresponding author.
E-mail address: wktiong@unimas.my (Wei King Tiong)

coastal marine construction [18]. Therefore, it is important to understand the behaviour of internal solitary waves.
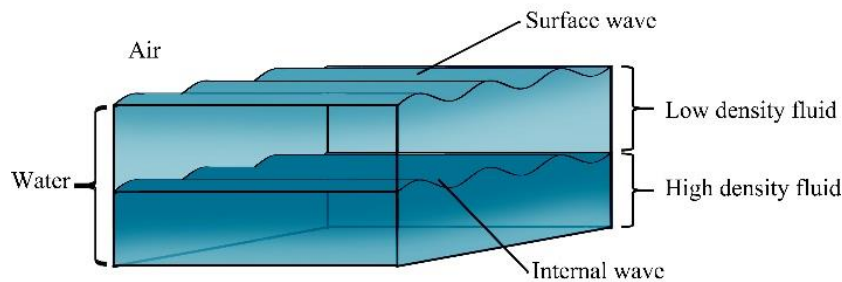
Fig. 1. Internal wave oscillates between two different density fluid layers

It is widely accepted that the propagation of internal solitary waves can be modelled using the Korteweg-de Vries (KdV) equation or KdV-type equations. The KdV equation was first used to model the evolution of internal solitary wave by Benney [19] and Benjamin [20] and followed by many other researchers [21-26]. Due to some real environmental conditions, internal waves often have a very small coefficient in nonlinear term with large amplitude propagating across the continental shelf area [27]. In order to balance the nonlinearity and dispersion effects, a cubic nonlinear term is added into the KdV equation [21]. Hence, the KdV equation is replaced by the extended Korteweg de Vries (eKdV) equation, or more commonly known as the Gardner equation. The canonical eKdV equation is given by

$$u_t + \alpha u u_x + \beta u^2 u_x + \lambda u_{xxx} = 0 \,, \tag{1}$$

where α, β, and λ are the coefficients that describe the behaviour of the waves and x, t are the temporal and spatial variables respectively. When the value of these coefficients are constant, then Eq. (1) has a steady-state solitary wave solution which is defined by

$$u(x,t) = \frac{A}{1+B \cosh K(x-Vt)} \,, \tag{2}$$

where

$$B^2 = 1 + \frac{6\lambda\beta K^2}{a^2}, \; V = \frac{aA}{6} = \lambda K^2 \tag{3}$$

From Eq. (2), the solution of the solitary wave is characterized by the single parameter B. The amplitude of the solitary wave is given by

$$u(x,t) = \frac{A}{1+B} \tag{4}$$

For $\lambda\beta < 0$, there is just a single branch of solutions with the range $0 < B < 1$. When $B \to 0$, the solution gives a limiting flat-topped wave which amplitude is limited to $-\alpha/\beta$, also known as "table-top" solitary wave. When $B \to 1$, the wave solution is small-amplitude KdV-type (sech^2-profile) solitary wave (see Figure 2(a)).

For $\lambda\beta > 0$, there are two branches of solutions which are divided into $1 < B < \infty$ and $-\infty < B < -1$. For $1 < B < \infty$, the solution gives a small-amplitude KdV-type solitary wave when $B \to 1$. When $B \to \infty$, the solution gives a large wave with a "sech²" profile (see the upper part of Figure 2(b)). The second branch $-\infty < B < -1$, it gives the solitary wave solution with negative polarity. When $B \to -1$, it gives a limiting algebra wave with the limited amplitude value of $-2\alpha/\beta$. The solution gives a negative large wave with a "sech²" profile when $B \to -\infty$ (see the lower part of Figure 2(b)) [28].

(a)   (b)
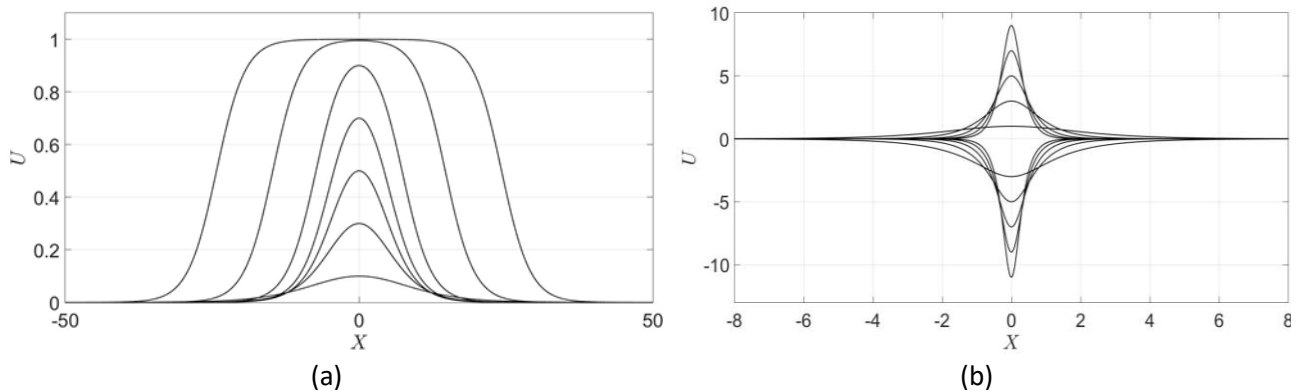
Fig. 2. The shape of solitary wave when (a) $\lambda\beta < 0$; (b) $\lambda\beta > 0$

In real-world ocean environment, internal solitary wave always propagates on the irregular ocean topography, e.g. continental shelves area and continental slope region. Also, there are many types of coastal structures have been built near the coastal area to reduce the impact of internal waves. Therefore, this paper intends at the effect of the variable topography on the evolution of the internal solitary wave.

In this paper, we consider internal solitary wave is propagating in a two-layer fluid system. When the internal solitary wave of depression propagates over a slowly changing topography, it exhibits a few interesting phenomena including the generation of solitary wavetrain, polarity change in the solitary wave, adiabatic and non-adiabatic deformations of the internal solitary wave depending on the nature of the slope [29].

The main aim of this paper is to look at the effect of rapidly varying topography on the internal solitary waves of depression. In Section 2, we shall present the formulation of our problem. Then in Section 3, we shall describe the numerical methods used to solve our problem. Then in Section 4, we shall present and discuss our numerical results followed by conclusion in the final section.

2. Problem Formulation

The appropriate mathematical model to describe the propagation of the internal solitary wave in a two-layer fluid system is the variable-coefficient eKdV (veKdV) equation [26], [28], [30, 31]. The veKdV equation has the following form

$$A_t + cA_x - \frac{cQ_x}{Q}A + \mu AA_x + \mu_1 A^2 A_x + \delta A_{xxx} = 0 \tag{5}$$

Here $A(x, t)$ is the amplitude of the solitary wave, and x, t are the temporal and spatial variables respectively. The coefficient $c(x)$ is the relevant linear long wave speed and $Q(x)$ is the linear modification factor, defined so that $Q^{-2}A^2$ is the wave action flux for linear long waves [28]. The

coefficients of the nonlinear and the dispersive term, i.e. $\mu(x)$, $\mu_1(x)$, and $\delta(x)$ are determined by the properties of the basic state of the fluid. All these coefficients are slowly-varying functions of x.

Let us consider the densities of the fluid in the upper layer and lower layer be constants denoted by ρ_1 and ρ_2 respectively. Also, consider H_1 is the depth of upper layer fluid and H_2 is the depth of lower layer fluid. The coefficients of Eq. (5) i.e. μ, μ_1 and δ are defined by

$$\mu = \frac{3c(\rho_2 H_1{}^2 - \rho_1 H_2{}^2)}{2H_1 H_2(\rho_2 H_1 + \rho_1 H_2)},$$

$$\mu_1 = \frac{-3c}{8(H_1{}^2 H_2{}^2)(\rho_1 H_2 + \rho_2 H_1)^2}\left[(\rho_1 H_2{}^2 - \rho_2 H_1{}^2)^2 + 8\rho_1 \rho_2 H_1 H_2 (H_1 + H_2)^2\right],$$

$$\delta = \frac{cH_1 H_2(\rho_1 H_1 + \rho_2 H_2)}{6(\rho_2 H_1 + \rho_1 H_2)}, \tag{6}$$

where

$$c = \sqrt{\frac{g(\rho_2 - \rho_1)H_1 H_2}{2\rho_1 H_2}}, \quad Q = \sqrt{\frac{1}{2g(\rho_2 - \rho_1)c}} \tag{7}$$

We shall suppose that the upper layer of the fluid has constant depth and the depth of the lower layer of the fluid varies rapidly according to

$$H_2(x) = h_0 \text{ for } x < x_0 \text{ and } H_2(x) = h_1 \text{ for } x > x_0,$$

where h_0 and h_1 are constants. Then, we shall suppose that the initial condition for Eq. (5) is imposed for $x \ll x_0$. The schematic of our problem is illustrated in Figure 3.
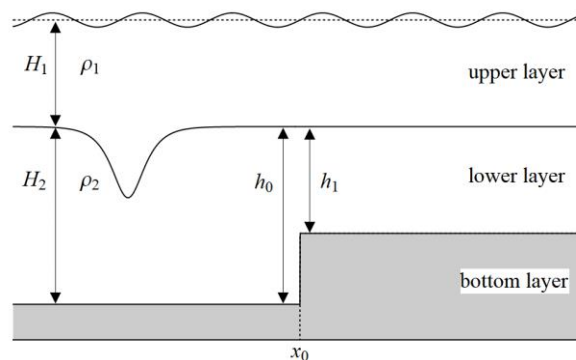
Fig. 3. Schematic illustration of ISW propagating in a two-layer medium of different density over a rapidly decreasing depth in the lower layer region

The first two terms in Eq. (5) are the dominants terms. Thus, we can make the transformation by introducing the following new variables [28]

$$A = QU, \qquad T = \int^x \frac{dx}{c}, \qquad X = c(T - t)$$

On substitution of the new variables into Eq. (5) gives, to the same leading order of approximation where Eq. (5) holds

$$U_T + \alpha U U_X + \beta U^2 U_X + \lambda U_{XXX} = 0, \tag{8}$$

where

$$U_T + \alpha U U_X + \beta U^2 U_X + \lambda U_{XXX} = 0, \tag{9}$$

In terms of the new variables $U(X, T)$, we consider that $H_1 = 1$ is constant for all T, $H_2(T) = h_0 = 1.5$ for $T < T_0$ and $H_2(T) = h_1$ when $T > T_0$.

3. Numerical Method

In order to solve Eq. (8), we apply the method of lines (MOL). Eq. (8) is reduced into a system of ordinary differential equations by making an approximation to the spatial derivatives, which will be solved by using the fourth-order Runge-Kutta method. The MOL is an ideal method which is widely used by many researchers to solve the partial differential equation such as the KdV equation [32, 33], the eKdV equation [34, 35], forced KdV equation [36] and forced KdV-Burgers equation [37].

Firstly, Eq. (8) is rewritten as

$$U_T = -\alpha U U_X - \beta U^2 U_X - \lambda U_{XXX} \tag{10}$$

Then we discretize the spatial derivatives using central finite difference formulas as follows

$$U_X \approx \frac{U_{j+1} - U_{j-1}}{2\Delta X},$$

$$U_{XXX} \approx \frac{U_{j+2} - 2U_{j+1} + 2U_{j-1} - U_{j-2}}{2(\Delta X)^3} \tag{11}$$

Here, j is the index that indicates the position along a spatial axis and ΔX is the increment value of spatial axis. Therefore, the MOL approximation of the Eq. (8) is given by

$$\frac{\partial U_j}{\partial T} = -\left(\alpha U_j + \beta[U_j]^2\right)\frac{U_{j+1} - U_{j-1}}{2\Delta X} - \lambda \frac{U_{j+2} - 2U_{j+1} + 2U_{j-1} - U_{j-2}}{2(\Delta X)^3},$$

$$= f(U_j). \tag{12}$$

For the time integration, we will use the fourth-order Runge-Kutta method. The initial condition is taken as

$$U(X, T = 0) = \frac{\alpha(B^2 - 1)}{\beta(1 + B\cosh(KX))}, \tag{13}$$

where

$$K = \sqrt{\frac{\alpha^2}{6\beta\lambda}(B^2 - 1)}. \tag{14}$$

Here, we consider two values for B, i.e. $B = 0.001$ and $B = 0.1$ in order to generate table-top solitary wave and KdV-type solitary wave with "sech^2" profile respectively.

4. Numerical Results

In this section, we shall present the numerical results for of the propagation of internal solitary wave for two different types of varying depth region, i.e. rapidly increasing and rapidly decreasing depth regions.

4.1 Rapidly Increasing Depth

In this subsection, we let the depth of the lower layer to be rapidly changing according to the following

$$H_2(T) = \begin{cases} 1.5 : 0 \leq T < 500, \\ 1.7 : T \geq 500, \end{cases}$$

Numerical simulations show that the initial internal solitary wave for both table-top solitary wave and KdV-type solitary wave disintegrates into two or more smaller internal solitary waves of the same polarity immediately as it propagates over the sharp step and followed by a small radiation wave behind it (see Figures 4 − 7). The size of the internal solitary wave generated after the slope is different from each other. This phenomenon is known as the fission of soliton [21]. This is because the coefficients $\alpha(T)$, $\beta(T)$, and $\lambda(T)$ in Eq. (8) make a rapid change from the value α_0, β_0, and λ_0 in the $T < T_0$ region to a new value α_1, β_1, and λ_1 in the $T > T_0$ region. The solitary wave solution in the region $T < T_0$ region is given by

$$U = \frac{\alpha_0 (B^2 - 1)}{\beta_0 (1 + B \cosh(KX))}, \tag{15}$$

where

$$K = \sqrt{\frac{\alpha_0^2}{6\beta_0\lambda_0}(B^2 - 1)}.$$

After T_0, the solitary wave enters the new constant depth region without change. However, the solitary wave solution Eq. (15) is no longer a solution for Eq. (8) when it enters new region at $T > T_0$, which has new constant coefficients α_1, β_1, and λ_1 in Eq. (8). As the result, the internal solitary wave fissions into N solitons and trailed by an oscillatory tail.

When $B = 0.001$, we have a table-top solitary wave of negative polarity or depression table-top solitary wave before the slope. The limiting amplitude of the table top solitary wave is given by

$$U_0 \approx -0.0909.$$

The first solitary wave generated after the slope is also a table-top solitary wave with new limiting amplitude

$$U_1 \approx -0.1257.$$
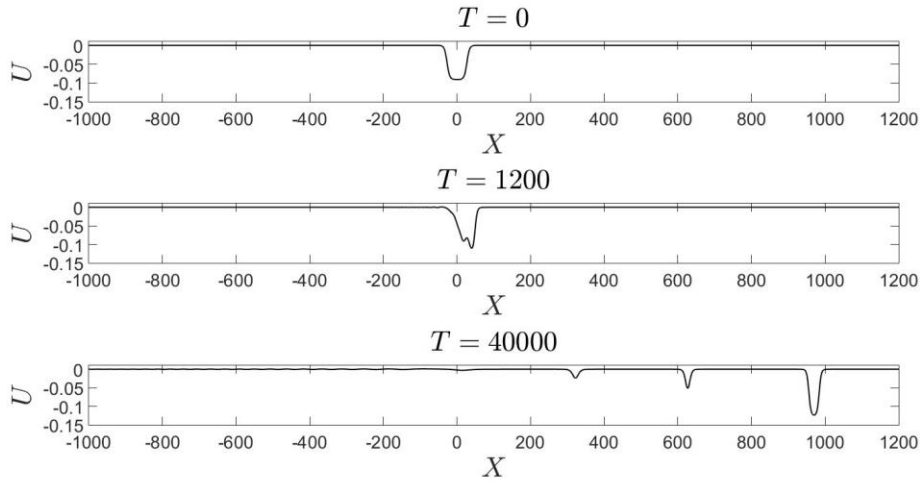
Fig. 4. 2D plots of a table-top solitary wave of negative polarity propagating over a rapidly decreasing slope
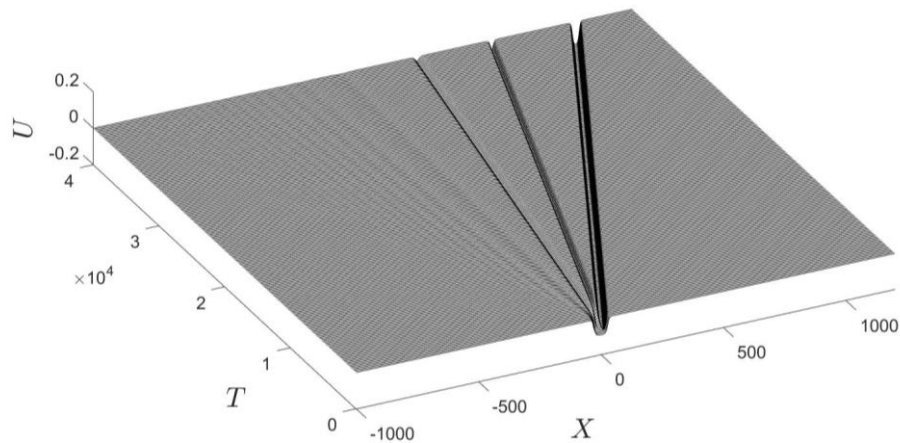
Fig. 5. 3D plot of a table-top solitary wave with negative polarity propagates over a rapidly decreasing slope
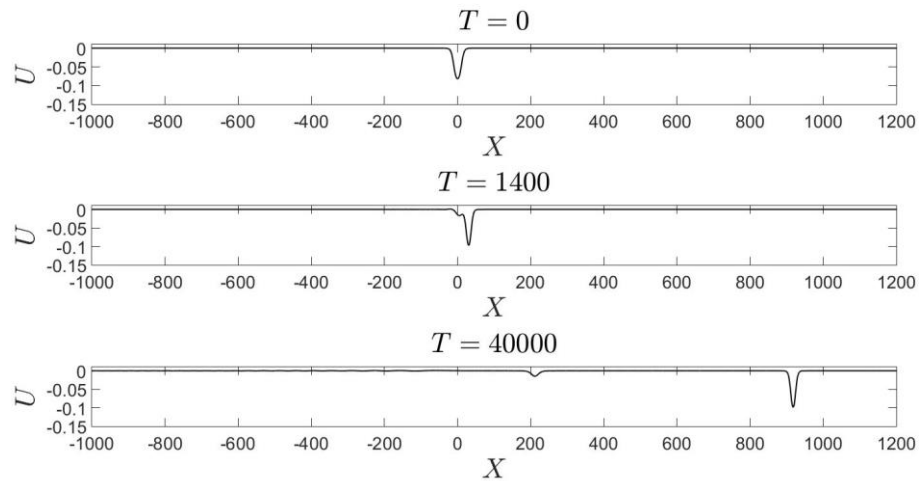
Fig. 6. 2D plots of a KdV-type solitary wave of negative polarity propagating over a rapidly decreasing slope
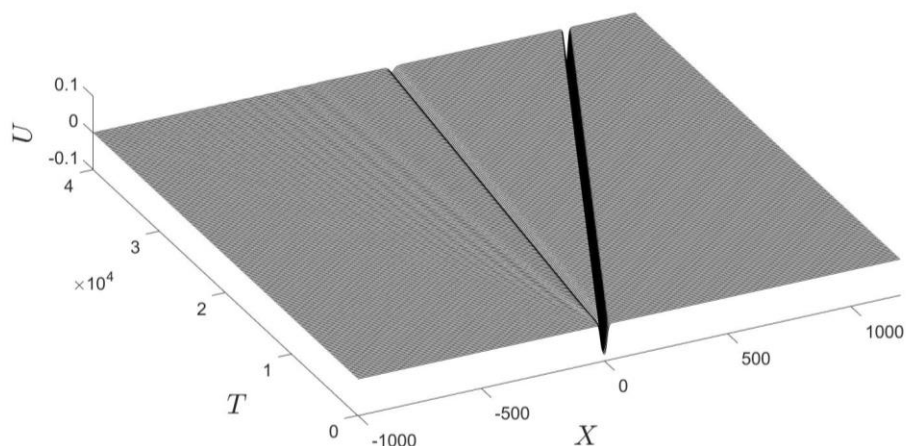
Fig. 7. 3D plot of a KdV-type solitary wave of negative polarity propagating over a rapidly decreasing slope

4.2 Rapidly Decreasing Depth

For rapidly decreasing depth, there are three different cases to be considered depending on the depth of the lower layer after the slope. First, we consider two cases, i.e.

a)   The depth of the lower layer is smaller than the depth of the upper layer

$$H_2(T) = \begin{cases} 1.5 : 0 \leq T < 500, \\ h_1 = 0.7 : T \geq 500. \end{cases}$$

b)   The depth of the lower layer is equivalent to the depth of the upper layer

$$H_2(T) = \begin{cases} 1.5 : 0 \leq T < 500, \\ h_1 = 1.0 : T \geq 500. \end{cases}$$

These two cases involve polarity change in Eq. (8), i.e. the sign of the coefficient α changes from negative, $\alpha < 0$, to a positive value, $\alpha > 0$, as it propagates over the sharp step. As a result of the sudden polarity changes in Eq. (8), the initial internal solitary wave of negative polarity becomes an initial disturbance to generate an undular bore of positive polarity riding on a pedestal. An undular bore is a nonlinear wavetrain connecting two different basic flow states and exhibits solitary wave of the leading edge and linear wave at the trailing edge [38-41]. This is clearly shown in 2D plots (see Figure 8 and Figure 9) and the 3D plots (see Figure 10 and Figure 11).

(a)

(b)
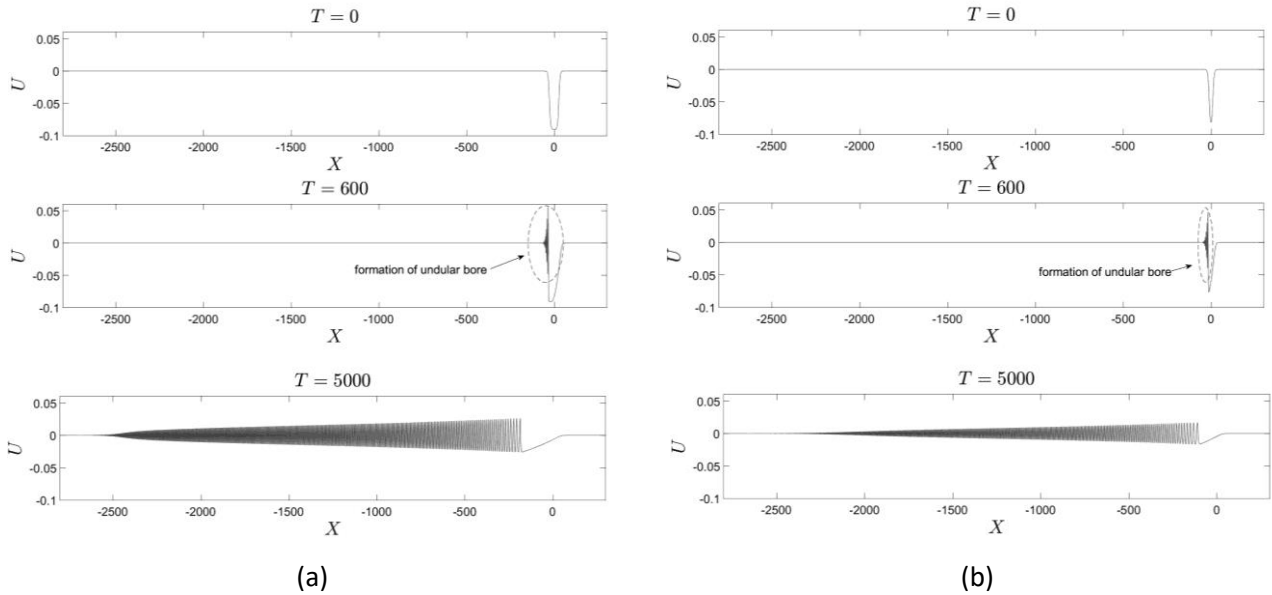
Fig. 8. 2D plots of (a) table-top solitary wave and (b) KdV-type solitary wave propagating over a rapidly increasing slope where $h_1 = 0.7$

(a)

(b)
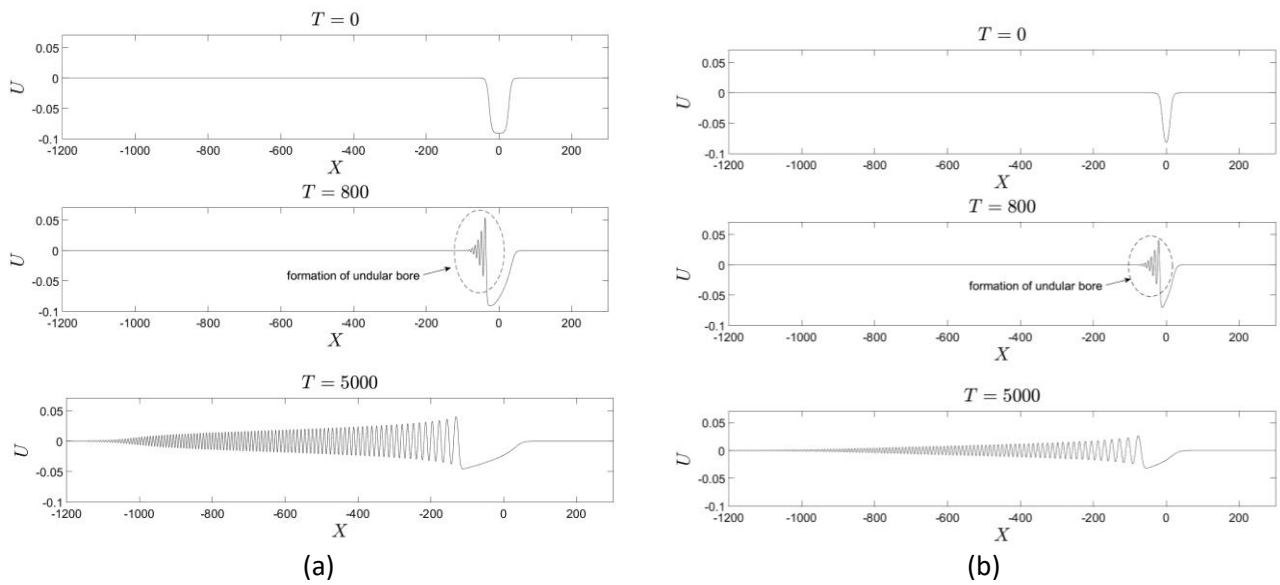
Fig. 9. 2D plots of (a) table-top solitary wave and (b) KdV-type solitary wave propagating over a rapidly increasing slope where $h_1 = 1.0$

(a)

(b)
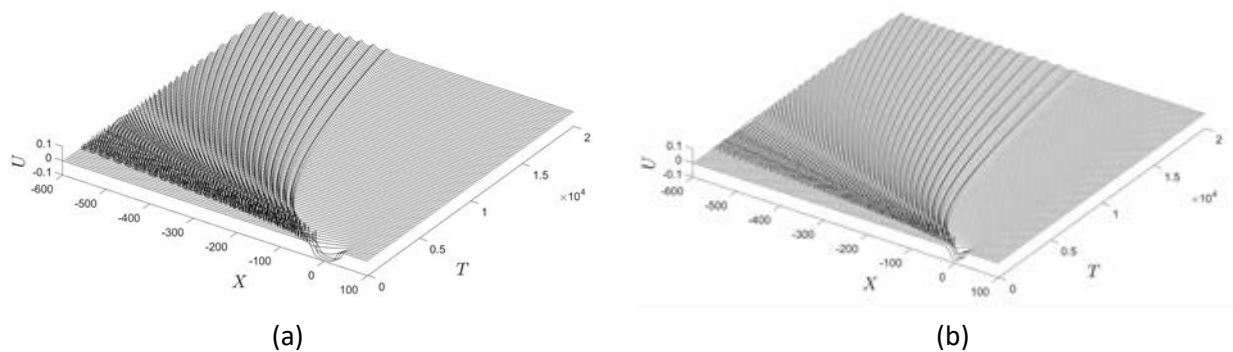
Fig. 10. 3D plots of (a) table-top solitary wave and (b) KdV-type solitary wave propagating over a rapidly increasing slope where $h_1 = 0.7$

(a)   (b)
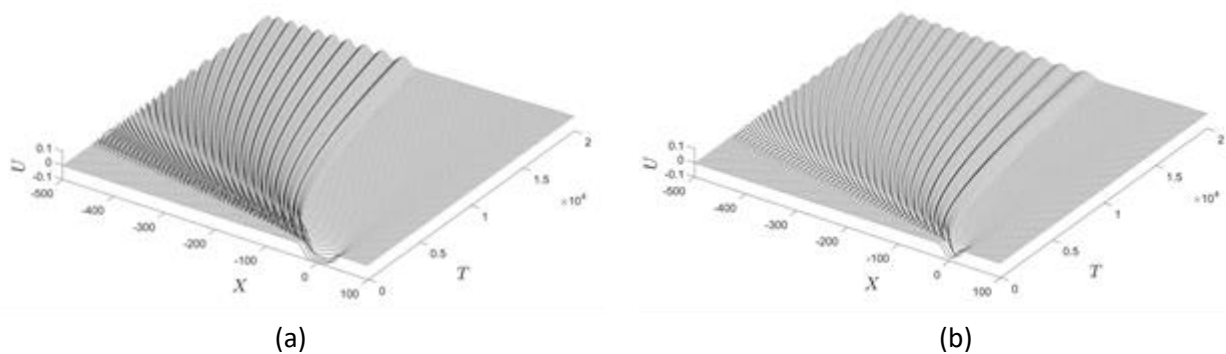
Fig. 11. 3D plots of (a) table-top solitary wave and (b) KdV-type solitary wave propagating over a rapidly increasing slope where $h_1 = 1.0$

On a large time-scale, the undular bore transforms into a linear wave due to the diminishing pedestal. As the result, the amplitude of leading solitary wave in the undular bore is decreasing over time. In other words, the internal solitary wave disperses as it propagates over the slope. Here, we only present the amplitude variations for table-top solitary wave (see Figure 12). The result is different if the slope is slowly varying. When the depth of the lower layer is smaller than the depth of the upper layer, a train of solitary waves of positive polarity is generated when the internal solitary waves of negative polarity are propagating over a slowly changing slope for both table-top and KdV-type solitary waves [29].

(a)   (b)
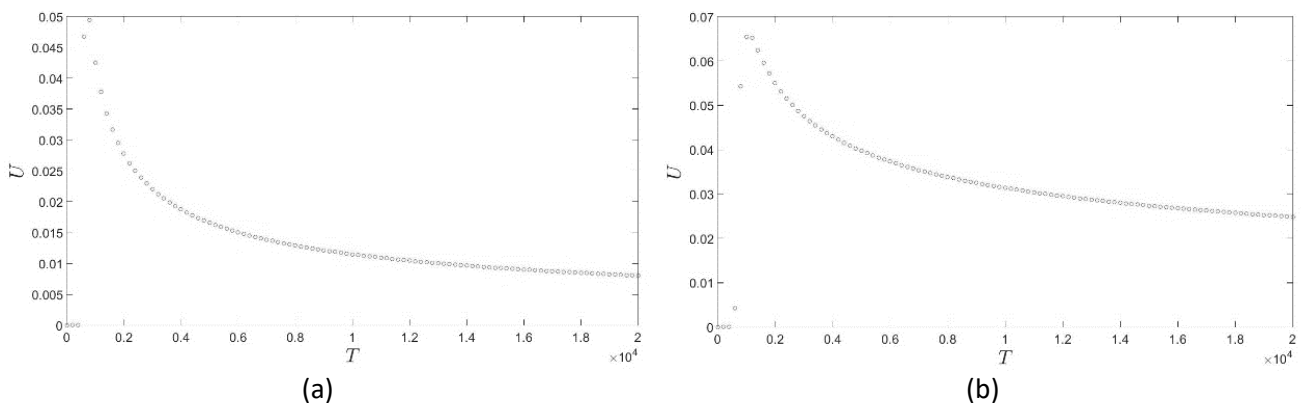
Fig. 12. Amplitude variation of the leading solitary wave in undular bore for (a) h_1=0.7; (b) h_1=1.0 for table-top solitary wave

Next, we consider the depth of the lower layer after the slope is greater than the upper layer. The depth profile is described by

$$H_2(T) = \begin{cases} 1.5 & : 0 \leq T < 500, \\ h_1 = 1.2 & : T \geq 500. \end{cases}$$

Unlike previous cases, we do not observe any polarity change here. From the numerical simulations, we observe that both table-top and KdV-type solitary waves transform into a new table-top solitary wave and followed by a radiation wave behind it (see Figures 13 – 15). The amplitude of the initial internal solitary wave decays and reaches a new limiting amplitude after the slope, which is given by

$U_1 \approx -0.03641.$
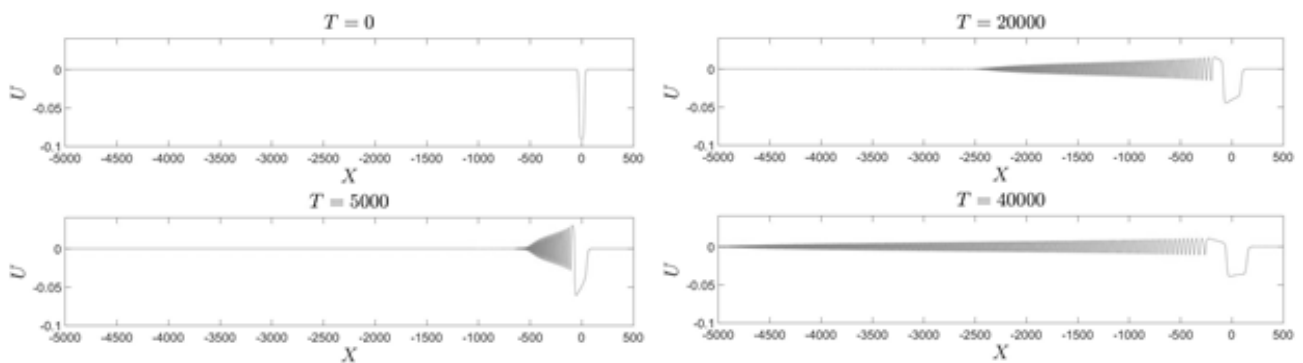
Fig. 13. 2D plots of a table-top solitary wave with negative polarity propagating over a rapidly increasing slope where h_1 = 1.2
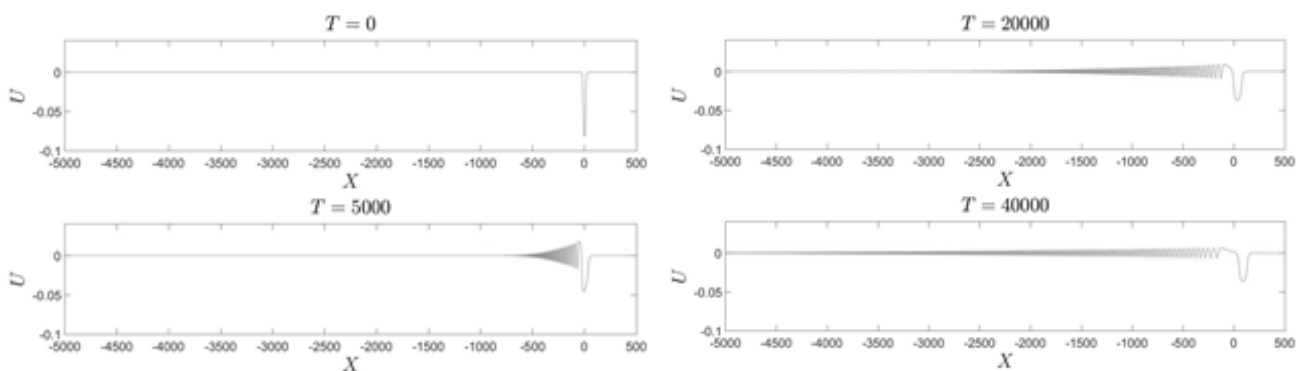
Fig. 14. 2D plots of a KdV-type solitary wave with negative polarity propagating over a rapidly increasing slope where h_1 = 1.2

(a)   (b)
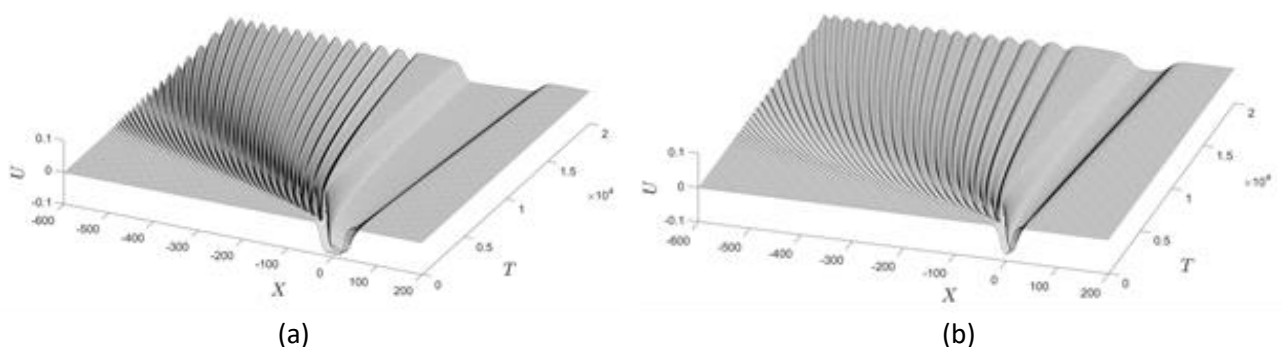
Fig. 15. 3D plots of (a) table-top solitary wave and (b) KdV-type solitary wave propagating over a rapidly increasing slope where h_1 = 1.2

5. Conclusions

In this paper, we have simulated the evolution of internal solitary wave over a sharply changing regions. If the depth of the lower layer is increasing rapidly, then the internal solitary wave fissions into several solitary waves of different sizes and of the same polarity. For the case when the depth of the lower layer is decreasing rapidly, the transformation of the internal solitary wave depends on the depth of the lower layer after the slope. If there is a polarity change, then the internal solitary

wave will act as a disturbance and generates an undular bore. However, the expansion of undular bore could not be supported over time due to the diminishing pedestal. Therefore, on a large time-scale, the undular bore transforms into a radiation wave. This observation is different from the case where the topography is changing slowly. Here we do not observe a generation of solitary wavetrain of positive polarity when the polarity changes. If there is not polarity change, the amplitude of the internal solitary wave decreases and produces a radiation wave. If the amplitude of the transformed internal solitary wave reaches the new limiting amplitude after the slope, then a table-top solitary wave would be generated. These results serve as a useful insight for the construction of underwater structures or buildings near the shores to prevent the impact of internal solitary waves on these structures.

References

[1]   Li, Xiaofeng, Zhongxiang Zhao, and William G. Pichel. "Internal solitary waves in the northwestern South China Sea inferred from satellite images." *Geophysical Research Letters* 35, no. 13 (2008): 1–7.
[2]   Saggio, Angelo, and Jörg Imberger. "Internal wave weather in a stratified lake." *Limnology and oceanography* 43, no. 8 (1998): 1780-1795.
[3]   Woodson, C. B., J. A. Barth, O. M. Cheriton, M. A. McManus, J. P. Ryan, L. Washburn, K. N. Carden et al. "Observations of internal wave packets propagating along-shelf in northern Monterey Bay." *Geophysical Research Letters* 38, no. 1 (2011): 1–6.
[4]   Sakai, Takahiro, and L. G. Redekopp. "A weakly nonlinear evolution model for long internal waves in a large lake." *Journal of Fluid Mechanics* 656 (2010): 260-297.
[5]   Støylen, Eivind, and Ilker Fer. "Tidally induced internal motion in an Arctic fjord." *Nonlinear Processes in Geophysics* 21, no. 1 (2014): 87–100.
[6]   Susanto, R. Dwi, Leonid Mitnik, and Quanan Zheng. "Ocean Internal Waves Observed in the Lombok Strait." *Oceanography* 18, no. 4 (2005): 80–87.
[7]   Nash, Jonathan D., and James N. Moum. "River plumes as a source of large-amplitude internal waves in the coastal ocean." *Nature* 437, no. 7057 (2005): 400–403.
[8]   Da Silva, J. C. B., A. L. New, M. A. Srokosz, and T. J. Smyth. "On the observability of internal tidal waves in remotely-sensed ocean colour data." *Geophysical Research Letters* 29, no. 12 (2002): 10–13.
[9]   Alpers, Werner. "Theory of radar imaging of internal waves." *Nature* 314, no. 6008 (1985): 245–247.
[10]   Osborne, A. R., and T. L. Burch. "Internal solitons in the Andaman Sea." *Science* 208, no. 4443 (1980): 451-460.
[11]   Liu, Antony K., James R. Holbrook, and John R. Apel. "Nonlinear internal wave evolution in the Sulu Sea." *Journal of Physical Oceanography* 15, no. 12 (1985): 1613-1624.
[12]   Grue, John. "Generation, propagation, and breaking of internal solitary waves." *Chaos: An Interdisciplinary Journal of Nonlinear Science* 15, no. 3 (2005): 037110.
[13]   Cai, Shuqun, Jieshuo Xie, and Jianling He. "An overview of internal solitary waves in the South China Sea." *Surveys in Geophysics* 33, no. 5 (2012): 927-943.
[14]   Chen, Ying-Jung, Dong Shan Ko, and Ping-Tung Shaw. "The generation and propagation of internal solitary waves in the South China Sea." *Journal of Geophysical Research: Oceans* 118, no. 12 (2013): 6578-6589.
[15]   Lien, Ren-Chieh, Frank Henyey, Barry Ma, and Yiing Jang Yang. "Large-amplitude internal solitary waves observed in the northern South China Sea: properties and energetics." *Journal of Physical Oceanography* 44, no. 4 (2014): 1095-1115.
[16]   Klymak, Jody M., Robert Pinkel, Cho-Teng Liu, Antony K. Liu, and Laura David. "Prototypical solitons in the south china sea." *Geophysical Research Letters* 33, no. 11 (2006).
[17]   Huang, Xiaodong, Zhaohui Chen, Wei Zhao, Zhiwei Zhang, Chun Zhou, Qingxuan Yang, and Jiwei Tian. "An extreme internal solitary wave event observed in the northern South China Sea." *Scientific reports* 6 (2016): 30041.
[18]   Osborne, A. R., T. L. Burch, and R. I. Scarlet. "The influence of internal waves on deep-water drilling." *Journal of Petroleum Technology* 30, no. 10 (1978): 1497–1504.
[19]   Benney, David John. "Long non-linear waves in fluid flows." *Journal of Mathematics and Physics* 45, no. 1-4 (1966): 52-63.
[20]   Benjamin, T. Brooke. "Internal waves of finite amplitude and permanent form." *Journal of Fluid Mechanics* 25, no. 2 (1966): 241-270.
[21]   Grimshaw, Roger, Efim Pelinovsky, and Tatjana Talipova. "Solitary wave transformation in a medium with sign-variable quadratic nonlinearity and cubic nonlinearity." *Physica D: Nonlinear Phenomena* 132, no. 1-2 (1999): 40-

62.

[22] Hamdi, Samir, Brian Morse, Bernard Halphen, and William Schiesser. "Analytical solutions of long nonlinear internal waves: Part I." *Natural Hazards* 57, no. 3 (2011): 597-607.

[23] Holloway, Peter, Efim Pelinovsky, and Tatiana Talipova. "Internal tide transformation and oceanic internal solitary waves." In *Environmental stratified flows*, pp. 29-60. Springer, Boston, MA, 2001.

[24] Apel, John R., Lev A. Ostrovsky, Yury A. Stepanyants, and James F. Lynch. "Internal solitons in the ocean and their effect on underwater sound." *The Journal of the Acoustical Society of America* 121, no. 2 (2007): 695-722.

[25] Helfrich, Karl R., and W. Kendall Melville. "Long nonlinear internal waves." *Annu. Rev. Fluid Mech.* 38 (2006): 395-425.

[26] Grimshaw, Roger, ed. *Environmental stratified flows*. No. 3. Springer Science & Business Media, 2002.

[27] Massel, Stanisław R. *Internal gravity waves in the shallow seas*. Springer International Publishing, 2015.

[28] Grimshaw, Roger, E. Pelinovsky, T. Talipova, and Oxana Kurkina. "Internal solitary waves: propagation, deformation and disintegration." *Nonlinear Processes in Geophysics* 17, no. 6 (2010): 633-649.

[29] Hooi, M. H., W. K. Tiong, K. G. Tay, S. N. Sze, and K. L. Chiew. "Simulation of internal solitary waves with negative polarity in slowly varying medium." In *AIP Conference Proceedings*, vol. 2013, no. 1, p. 020006. AIP Publishing, 2018.

[30] Grimshaw, Roger. "Internal solitary waves in a variable medium." *GAMM-Mitteilungen* 30, no. 1 (2007): 96-109.

[31] Grimshaw, Roger, Efim Pelinovsky, Tatiana Talipova, and Audrey Kurkin. "Simulation of the transformation of internal solitary waves on oceanic shelves." *Journal of Physical Oceanography* 34, no. 12 (2004): 2774-2791.

[32] Schiesser, William E. *The numerical method of lines: integration of partial differential equations*. Elsevier, 2012.

[33] Schiesser, W. E. "Method of lines solution of the Korteweg-de Vries equation." *Computers & Mathematics with Applications* 28, no. 10-12 (1994): 147-154.

[34] Marchant, T. R., and N. F. Smyth. "Soliton interaction for the extended Korteweg-de Vries equation." *IMA Journal of Applied Mathematics* 56, no. 2 (1996): 157-176.

[35] Tiong, W. K., K. G. Tay, C. T. Ong, and S. N. Sze. "Numerical Solution of the Gardner Equation." In *Proceedings of the International Conference on Computing, Mathematics and Statistics (iCMS 2015)*, pp. 243-251. Springer, Singapore, 2017.

[36] Yazid, Nazatulsyima Mohd, Kim Gaik Tay, Yaan Yee Choy, Azila Md Sudin, Wei King Tiong, and Chee Tiong Ong. "Numerical Solution of the Forced Korteweg-de Vries (FKDV) Equation." *ARPN Journal of Engineering and Applied Sciences* 11, no. 18 (2016): 10757–10760.

[37] Yazid, Nazatulsyima Mohd, Kim Gaik Tay, Wei King Tiong, Yaan Yee Choy, Azila Md Sudin, and Chee Tiong Ong. "The method of lines solution of the Forced Korteweg-de Vries-Burgers equation." *Matematika* 33, no. 1 (2017): 35-41.

[38] Smyth, N. F., and P. E. Holloway. "Hydraulic jump and undular bore formation on a shelf break." *Journal of Physical Oceanography* 18, no. 7 (1988): 947-962.

[39] El, G. A., Roger HJ Grimshaw, and Noel F. Smyth. "Unsteady undular bores in fully nonlinear shallow-water theory." *Physics of Fluids* 18, no. 2 (2006): 027104.

[40] Esler, J. G., and J. D. Pearce. "Dispersive dam-break and lock-exchange flows in a two-layer fluid." *Journal of Fluid Mechanics* 667 (2011): 555-585.

[41] El, G. A., Roger HJ Grimshaw, and Wei K. Tiong. "Transformation of a shoaling undular bore." *Journal of Fluid Mechanics* 709 (2012): 371-395.